

1.4 Bentonites other than MX-80

Mattias Åkesson

Clay Technology AB, Lund, Sweden

November 2013

Contents

1	Introduction.....	3
1.1	Background.....	3
1.2	Scope.....	3
2	Hydraulic conductivity.....	4
3	Swelling pressure.....	6
4	Retention properties.....	8
5	Water uptake tests.....	9
6	Thermal conductivity.....	11
7	Evaluation of hydraulic properties.....	12
7.1	Diffusivity evaluation from water-uptake tests.....	12
7.2	Diffusivity evaluation from hydraulic conductivity and initial RH.....	13
8	Homogenization processes.....	19
8.1	Homogenization calculations in SR-Site.....	19
8.2	Homogenization tests.....	19
9	Concluding remarks.....	21
	References.....	22
	Appendix - Water-uptake tests with Febex bentonite.....	24

1 Introduction

1.1 Background

SKB has been asked to comment the fact that different bentonite types may be more or less favourable in the perspective of the resaturation phase.

1.2 Scope

The aim of this analysis was: i) to present the available data concerning hydro-mechanical properties for bentonites other than MX-80; and ii) to evaluate whether these properties can lead to other modelling results than those which were presented in SR-Site.

With available data is primarily meant results from measurement of hydraulic conductivity, swelling pressure, retention properties and from water uptake tests. In addition, data on thermal conductivity and some results from homogenization test are also included in the presentation. With bentonites other than MX-80 is primarily meant Deponit Ca-N, Ibeco RWC BF, Asha, Friedland and Febex. A compilation of sources of hydro-mechanical data for different bentonites is shown in Table 1-1.

A simple way to estimate the water-uptake capacity for different materials is to evaluate the moisture diffusivity from water uptake tests. Moisture diffusivities can also be evaluated from hydraulic conductivity values and retention properties. The consistency between different data sets can in this way be corroborated, while the material model can be verified from independent measurements.

Table 1-1. Sources of hydro-mechanical data for different bentonites.

Bentonite	Hydraulic conductivity	Swelling pressure	Retention properties	Water-uptake test	Thermal cond.	Homogen. test
MX-80	Relation: TR-10-44	Relation: TR-10-44	TR-10-55 Dueck 2004	IPR-01-34	Relations: TR-10-44	-
Deponit Ca-N	TR-06-30 TR-11-06	TR-06-30 TR-11-06	-	-	-	-
Asha	TR-06-30 TR-11-06	TR-06-30 TR-11-06	R-08-136	R-08-136	-	-
Ibeco RWC BF	R-13-08 R-10-44	R-13-08 R-10-44	R-10-44	R-10-44	-	R-10-44
Friedland	TR-06-30 R-08-136	TR-06-30 R-08-136	R-08-136	R-08-136	-	R-08-136
Febex	Villar 2002	Villar 2002	Villar 2002	This study	Villar 2002	-

* Tests with same material for block and pellets

2 Hydraulic conductivity

Hydraulic conductivity data for different materials have been reported from a number of studies: Karnland et al. (2006) (TR-06-30) presented results for a large number of bentonites, among which the data for Friedland, Deponit Ca-N and Asha (Kutch) are of interest in this study; Johannesson et al. (2010) (R-10-44) presented results for Ibeco RWC BF; Svensson et al. (2011) (TR-11-06) presented results for reference material of Asha and Deponit Ca-N; Sandén et al. (2013) (R-13-08) presented results for Ibeco RWC BF and Asha (two different shipments); finally, Villar (2002) presented results for Febex. All data from these analyses (dry density higher than 1000 kg/m^3) are compiled in Figure 2-1. A relation adopted for MX-80 data by Åkesson et al. (2010a) (TR-10-44) is shown for comparison. For a dry density level of $1500\text{-}1600 \text{ kg/m}^3$ the following approximate observations can be made:

- For Friedland material, the hydraulic conductivity values were more than one order of magnitude higher than for MX-80;
- For Asha (in three different studies) and for Ibeco RWC BF (in one study), the hydraulic conductivity values were 2-3 times higher than for MX-80;
- Deponit Ca-N, Ibeco RWC BF (in one study) and Febex material displayed approximately the same hydraulic conductivity values as MX-80;
- Finally for Asha (in one study) the hydraulic conductivity values were 2-3 times lower than for MX-80.

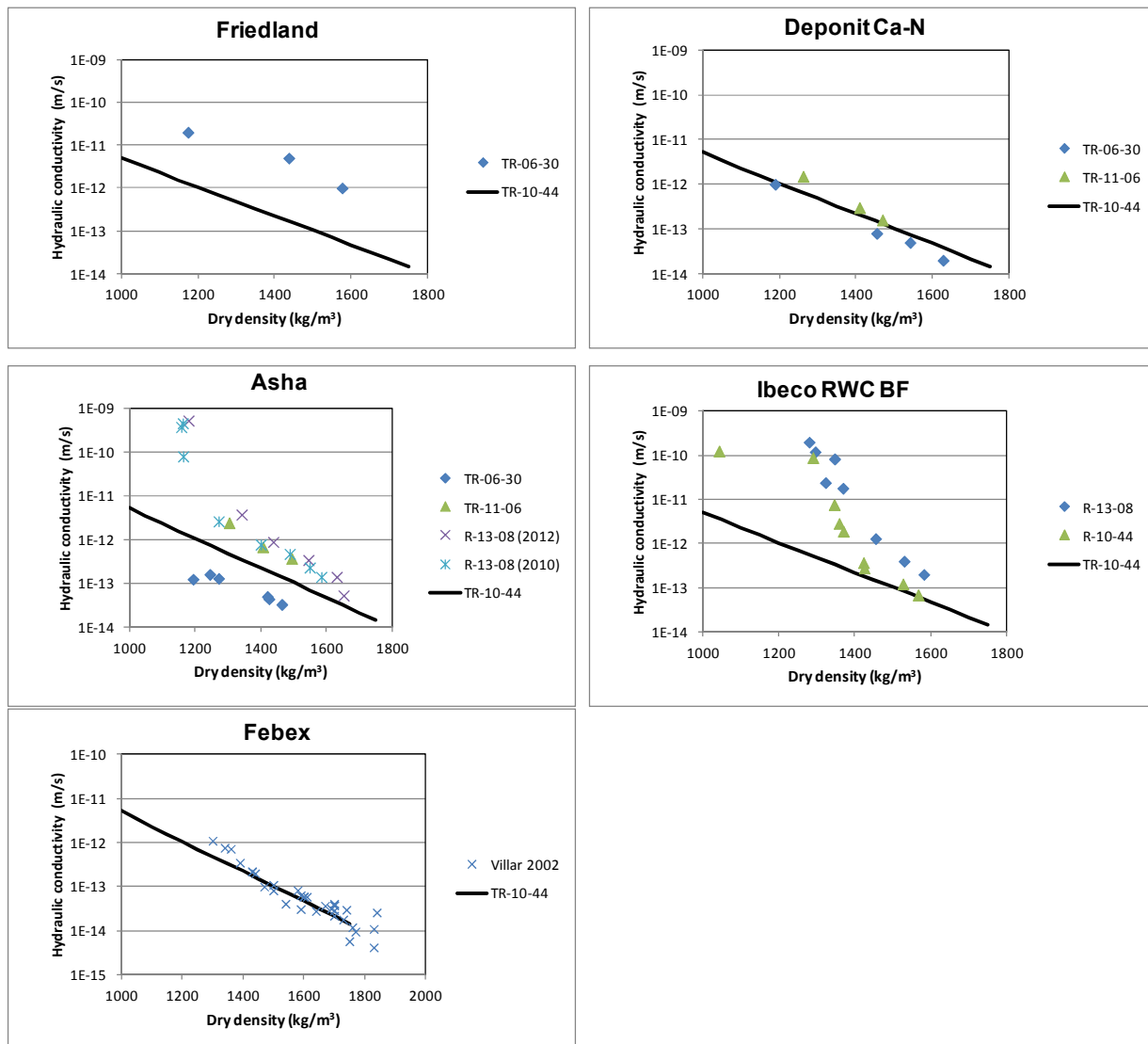


Figure 2-1. Hydraulic conductivity data for different materials. A relation adopted for MX-80 data (marked TR-10-44) is shown for comparison.

3 Swelling pressure

Swelling pressure data for different materials have been reported from a number of studies: Karnland et al. (2006) (TR-06-30) presented results for a large number of bentonites, among which the data for Friedland, Deponit Ca-N and Asha (Kutch) are of interest in this study; Johannesson et al. (2010) (R-10-44) presented results for Ibeco RWC BF; Svensson et al. (2011) (TR-11-06) presented results for reference material of Asha and Deponit Ca-N; Sandén et al. (2013) (R-13-08) presented results for Ibeco RWC BF and Asha (two different shipments); Johannesson and Börgesson 2002 (IPR-02-50) presented results from oedometer tests on Friedland; finally, Villar (2002) presented results for Febex. All data from these analyses (dry density higher than 1000 kg/m^3) is compiled in Figure 3-1. A relation adopted for MX-80 data by Åkesson et al. (2010a) (TR-10-44) is shown for comparison. For a dry density level of 1500-1600 kg/m^3 the following approximate observations can be made:

- For Friedland material, the swelling pressure values were one order of magnitude lower than for MX-80;
- For Ibeco RWC BF (in one study), the swelling pressure values were 2-3 times lower than for MX-80;
- Asha (in three different studies), Deponit Ca-N, Ibeco RWC BF (in one study) and Febex material displayed approximately the same swelling pressure values as MX-80;
- Finally for Asha (in one study), the swelling pressure values were 2-3 times higher than for MX-80.

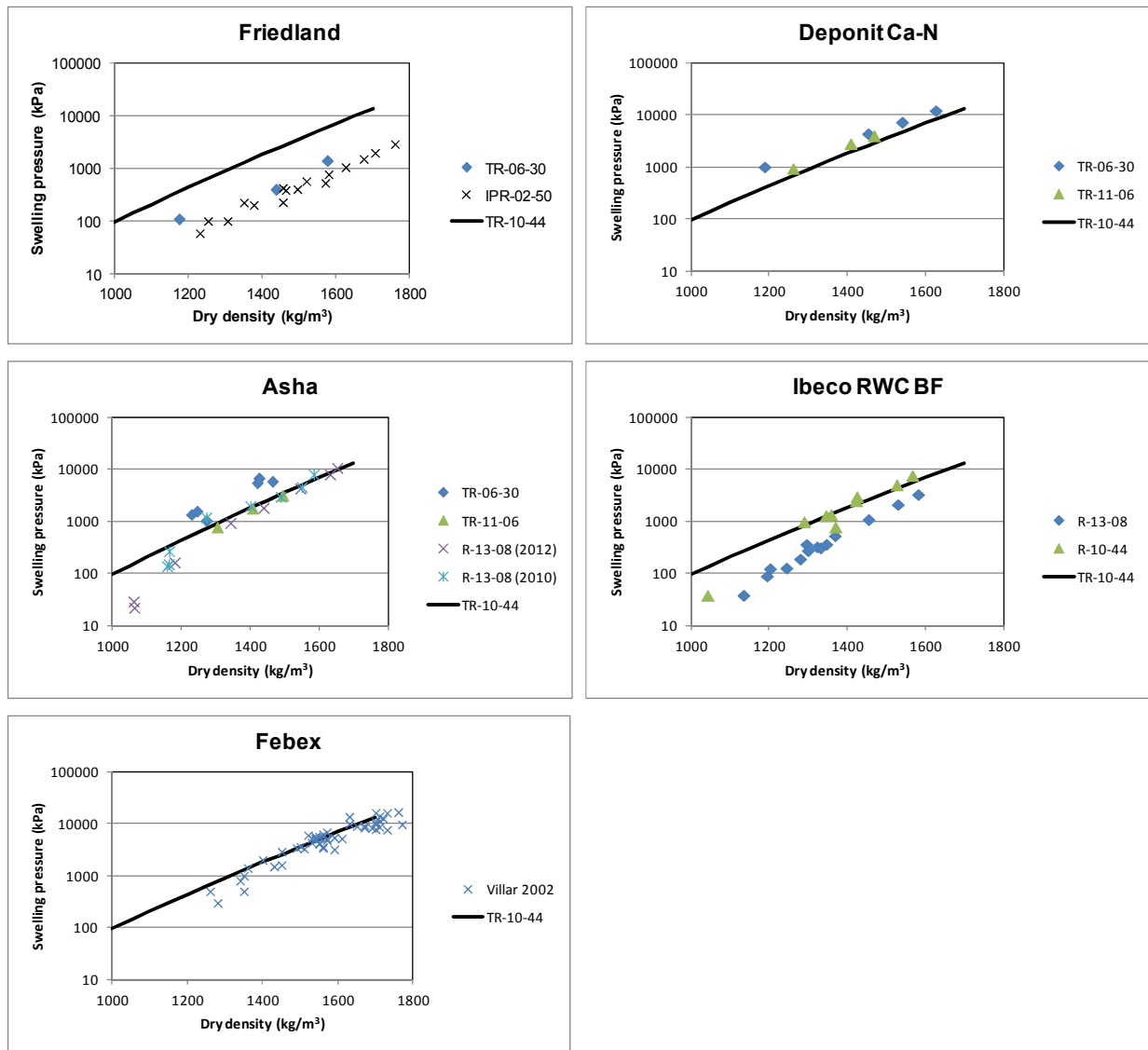


Figure 3-1. Swelling pressure data for different materials. A relation adopted for MX-80 data (marked TR-10-44) is shown for comparison.

4 Retention properties

Water retention data for different materials have been reported from a number of studies: Johannesson et al. (2008) (R-08-136) presented results for Asha and Friedland; Johannesson et al. (2010) (R-10-44) presented results for Ibeco RWC BF; finally, Villar (2002) presented results for Febex. All data from these analyses, i.e. water content versus relative humidity (RH), are compiled in Figure 4-1. In addition, two sets of data for MX-80, presented by Dueck and Nilsson (2010) (TR-10-55) and Dueck (2004) are shown for comparison.

For an approximate level of water content of 17% the following observations can be made:

- Febex, Asha & Ibeco RWC BF equilibrate at a lower RH than MX-80,
- Friedland equilibrates at a higher RH than MX-80;

For an approximate level of water content of 25% the following observations can be made:

- Asha equilibrates at a lower RH than MX-80,
- Febex and Ibeco RWC BF equilibrate at approximately the same RH as MX-80,
- Friedland equilibrates at a higher RH than MX-80.

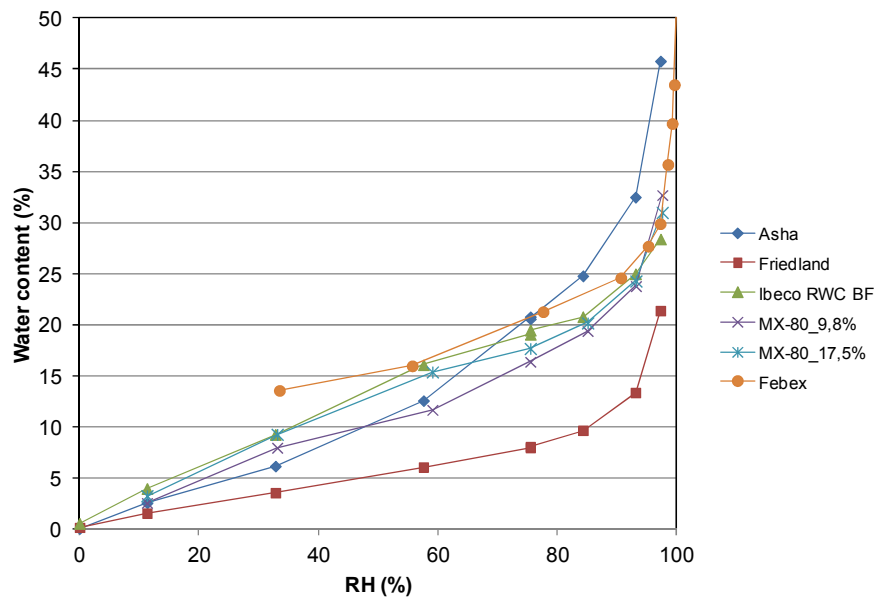


Figure 4-1. Retention data for different materials.

5 Water uptake tests

Water uptake tests have been reported from a number of studies: Börgesson (2001) (IPR-01-34) presented results for MX-80; Johannesson et al. (2008) (R-08-136) presented results for Asha and Friedland; and Johannesson et al. (2010) (R-10-44) presented results for Ibeco RWC BF. Results from these tests are compiled in Figure 5-1 to Figure 5-3. Finally, two water uptake tests were performed on Febex benonite within this study, see the Appendix. An evaluation of the results from all the tests is presented in Chapter 7.

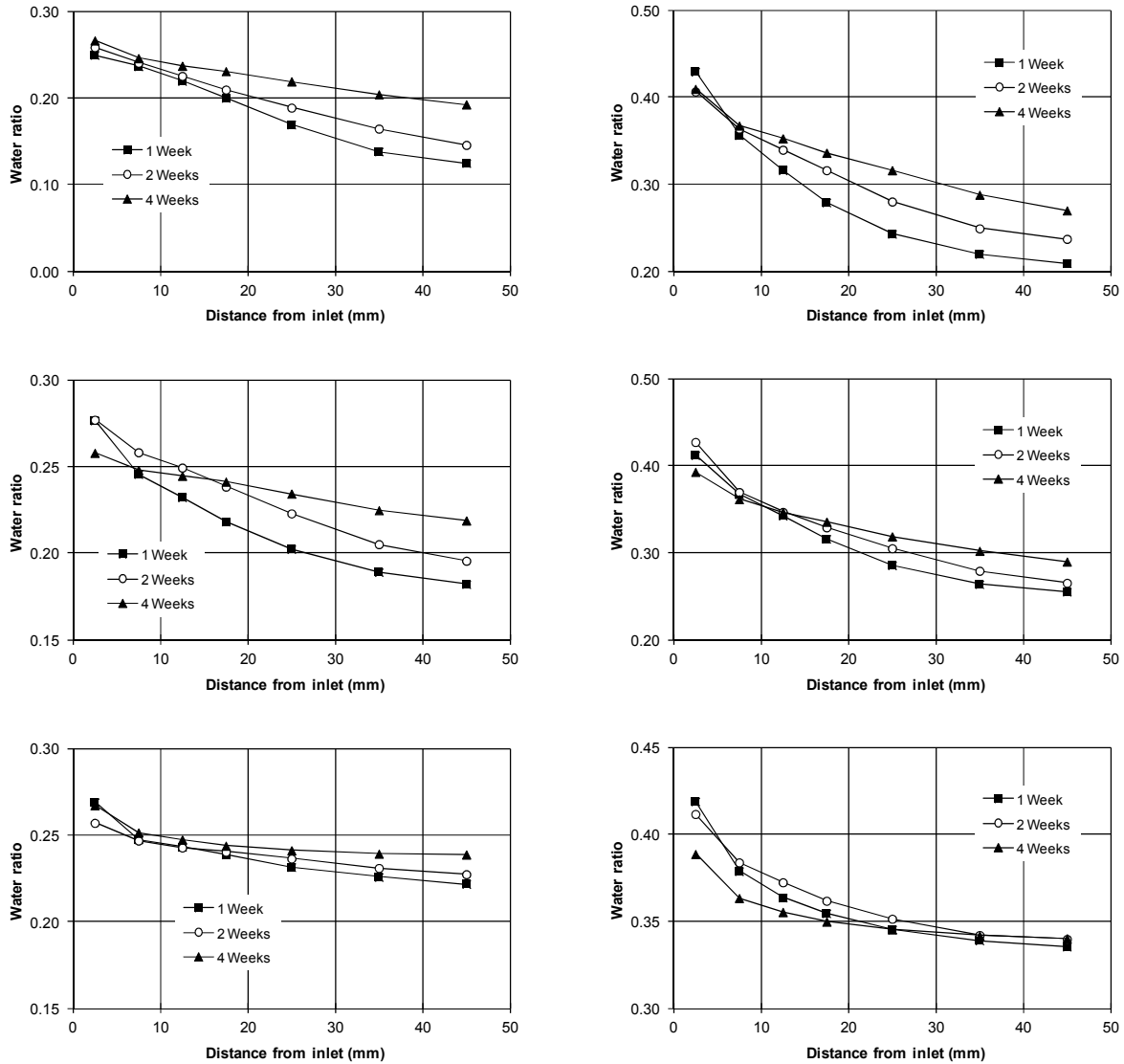


Figure 5-1. Water-uptake tests: MX-80.

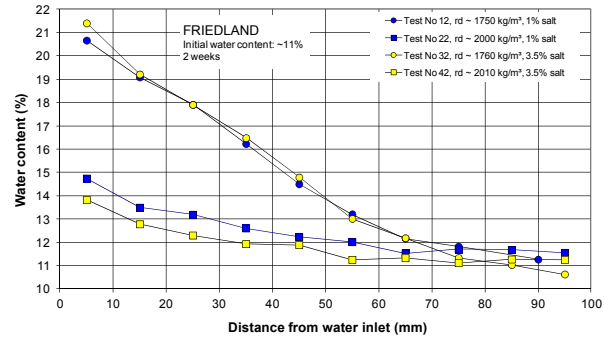
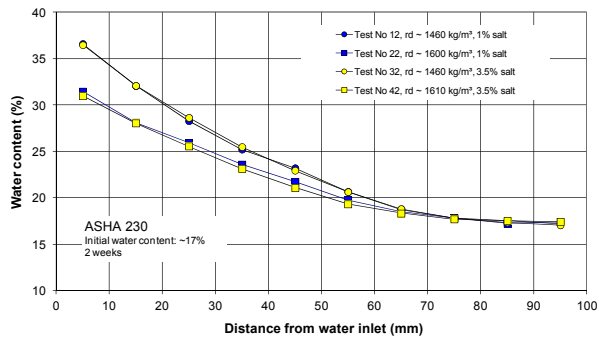
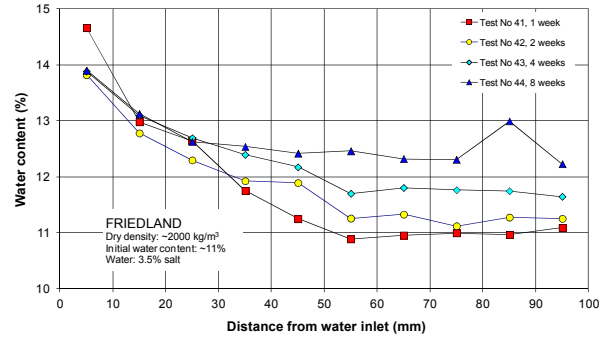
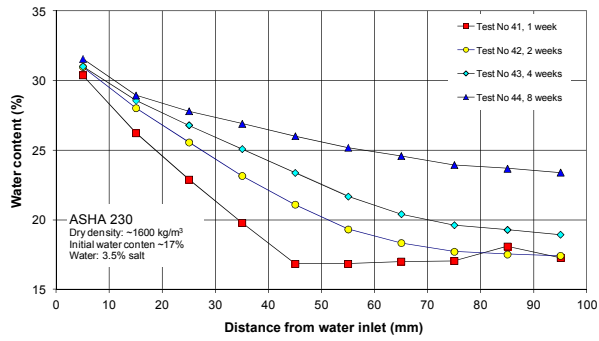
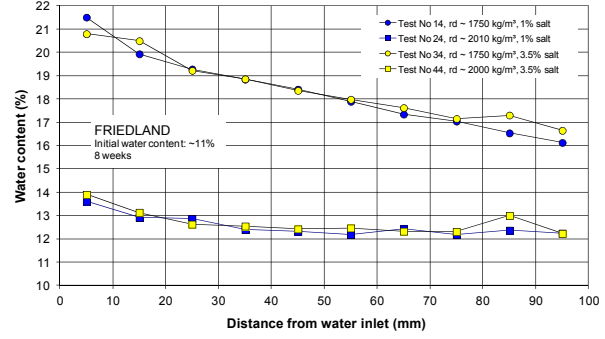
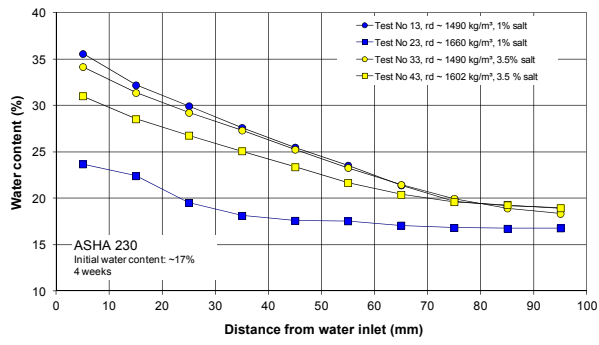


Figure 5-2. Water-uptake tests: Asha (left); Friedland (right).

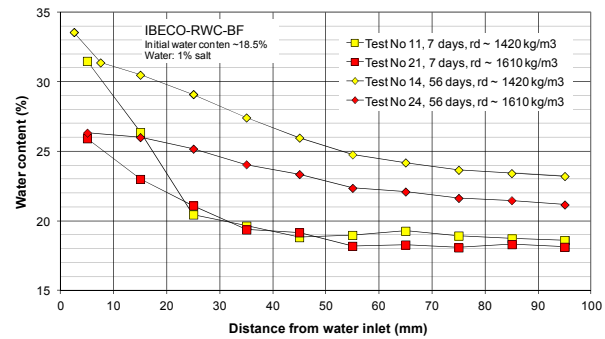
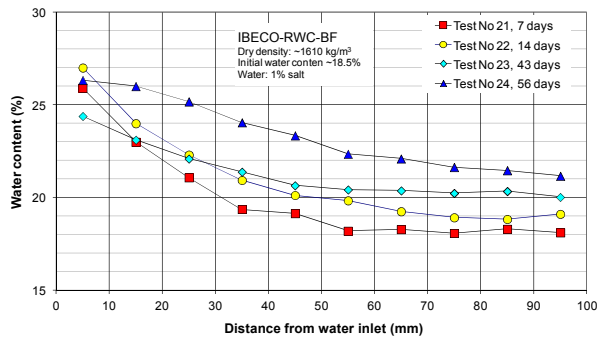


Figure 5-3. Water-uptake tests: Ibeco RWC BF.

6 Thermal conductivity

Thermal conductivity data has been reported from measurements performed by Villar (2002) on Febex bentonite. The data from this analysis is compiled in Figure 6-1 as a function of the degree of saturation. Three different relations adopted for MX-80 data by Åkesson et al. (2010a) (TR-10-44) are shown for comparison. The Febex data are generally quite similar to the MX-80 data relations, although the relations tend to overestimate the thermal conductivity at mid- saturation range, and underestimate the thermal conductivity at low saturation degrees.

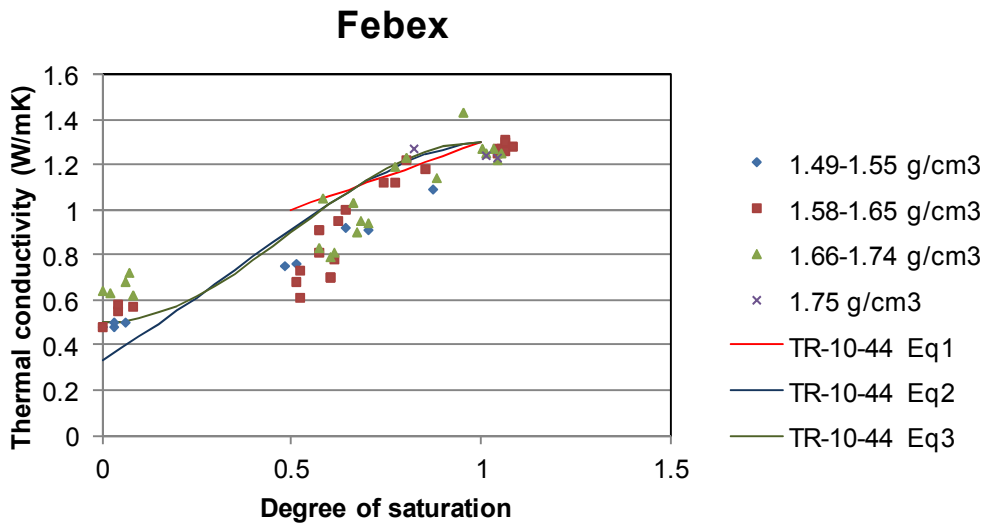


Figure 6-1. Thermal conductivity. Adopted functions for MX-80 (lines) and experimental data for Febex (symbols).

7 Evaluation of hydraulic properties

7.1 Diffusivity evaluation from water-uptake tests

Diffusivity (D) values were evaluated from the water-uptake tests presented in Chapter 5 and the Appendix. Each evaluation was based on three different water contents (Figure 7-1, left): initial value (w_i), boundary value (w_f), and temporal value (w_x) at a specified time and coordinate. The initial value was generally measured with adequate precision. Different approaches can be applied for the boundary value, such as the calculated from the average dry density of the specimen, or from the measured water content in the sample adjacent to the water inlet. The latter approach was applied in this analysis. The temporal value was based on one specific measurement.

The evaluations were based on an analytical solution for diffusion in a plane sheet (Crank, 1975):

$$\frac{w - w_i}{w_f - w_i} = 1 - \frac{4}{\pi} \sum_{n=0}^{\infty} \frac{(-1)^n}{2n+1} \exp \left\{ -D(2n+1)^2 \frac{\pi^2 t}{4l^2} \right\} \cos \frac{(2n+1)\pi x}{2l} \quad (7-1)$$

where t is the time, l is the length of the specimen, and x is the distance from the hydrated boundary, and a diffusivity value was sought with this function for each set of specified water contents. In order to optimize the precision, the samples used for the temporal values (w_x) were chosen as distant as possible from the hydrated boundary. Moreover, only tests for which the increase in water content ($w_x - w_i$) exceeded 1% were included in the evaluation. This was thus a very simple evaluation technique, which yielded only one constant D value from each test.

Evaluated moisture diffusivity values are plotted versus the temporal water contents (w_x) in Figure 7-1 (right). It can be noted that the evaluated diffusivity values are well-defined and display a fairly small variability. The values for Friedland ($6.5 - 8.4 \cdot 10^{-10} \text{ m}^2/\text{s}$) are clearly higher than all the other materials, whereas the values for and Asha, Febex and to some extent also Ibeco RWC BF ($5.1 - 6.7 \cdot 10^{-10} \text{ m}^2/\text{s}$) is higher than MX-80 at $e=0.7$ ($3.6 - 5.3 \cdot 10^{-10} \text{ m}^2/\text{s}$).

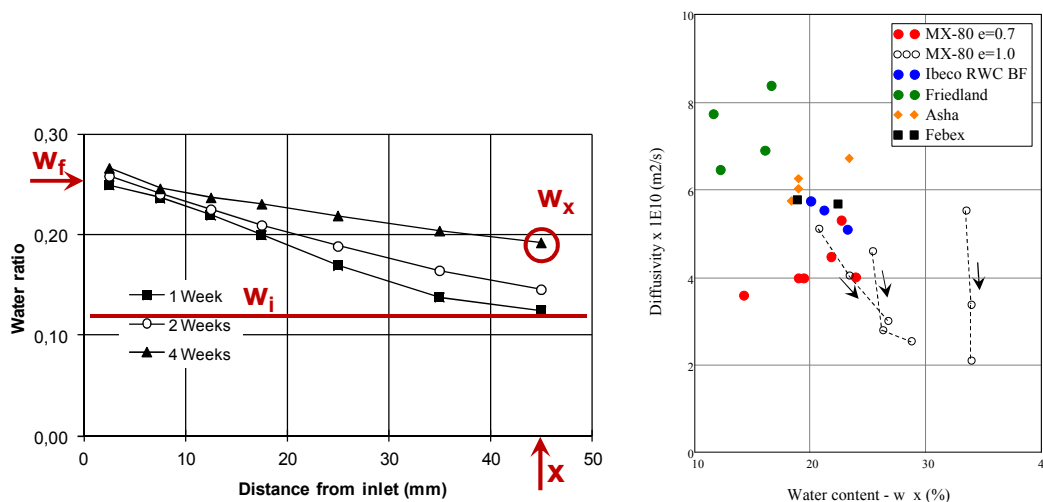


Figure 7-1. Water-uptake tests (left); evaluated diffusivity values (right).

The diffusivity values from tests performed on specimen with high density MX-80 ($e=0.7$) exhibit an increasing trend for increasing water content, which is consistent with other studies (Kahr et al. 1986). However, tests performed on low density MX-80 specimen ($e=1.0$) rather indicate that the diffusivity value tends to decrease at increasing water contents. Similar trends were found in a theoretical analysis of moisture diffusivities for unsaturated conditions (Börgesson et al. 2013).

7.2 Diffusivity evaluation from hydraulic conductivity and initial RH

The moisture diffusivity can be evaluated as a function of the saturation degree from the intrinsic permeability, k , the relative permeability relation, $k_r(S_l)$, the derivative of the retention curve, dP_l/dS_l , a homogenous porosity, n , and the water viscosity, μ :

$$D(S_l) = \frac{k \cdot k_r(S_l)}{n \cdot \mu} \cdot \frac{dP_l}{dS_l} \quad (m^2 / s) \quad (7-2)$$

A commonly used type of retention curve is the van Genuchten function:

$$S_l(P_l) = \left(1 + \left(\frac{P_g - P_l}{P_0} \right)^{1-\lambda} \right)^{-\lambda} \quad (7-3)$$

Two such curves were adopted for backfill blocks (Åkesson et al. 2010a) and were subsequently used for hydration calculations and evaluations of moisture diffusivity functions (Åkesson et al. 2010b), see Base case and Modified case in Figure 7-2. An alternative retention curve is the square law:

$$S_l(P_l) = \frac{1}{\sqrt{1 + \frac{P_g - P_l}{P_0}}} \quad (7-4)$$

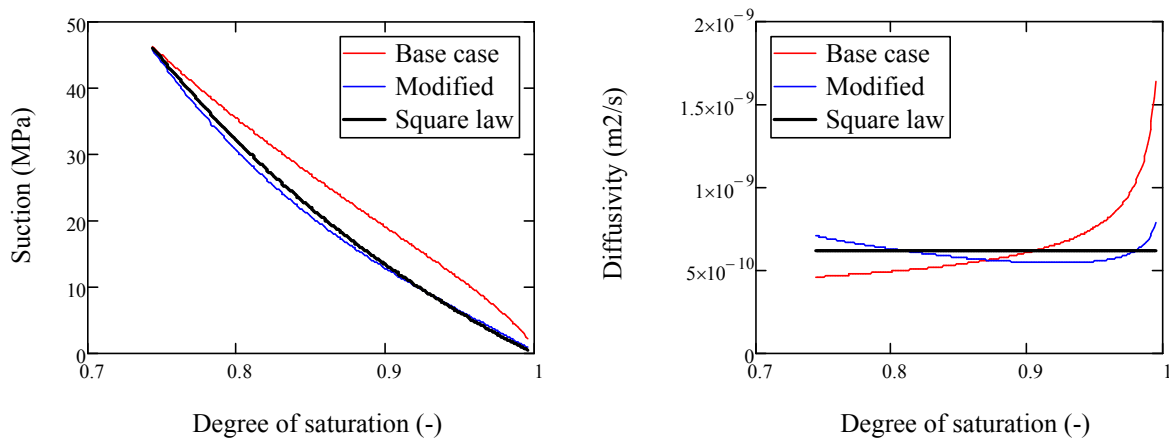


Figure 7-2. Retention curves, adopted for backfill blocks of MX-80 (left), and evaluated diffusivity relations (right).

This function is implemented in Code_Bright, and in combination with the cubic power law for the relative permeability it implies a *constant diffusivity value*. Such a curve is illustrated in Figure 7-2 with the same initial point as for the backfill blocks. It can be noted that the square law only has one parameter and that this is specified as soon as the initial point is defined.

The inverse function of square law can be expressed as:

$$P_l(S_l) = P_g - P_0 \cdot \left(\frac{1}{S_l^2} - 1 \right) \quad (7-5)$$

The derivative of this function is simply:

$$\frac{dP_l}{dS_l} = \frac{2P_0}{S_l^3} \quad (7-6)$$

The sole parameter P_0 is specified from the initial point (ψ_{init} , S_{init}):

$$P_0 = \frac{P_g - P_l}{\frac{1}{S_l^2} - 1} = \frac{\psi_{init}}{\frac{1}{S_{init}^2} - 1} \quad (7-7)$$

The expressions for the derivative (7-6) and the parameter (7-7) can be substituted in the evaluation of diffusivity (7-1):

$$D = \frac{k \cdot S_l^3}{n \cdot \mu} \cdot \frac{2P_0}{S_l^3} = \frac{2k}{n \cdot \mu} \cdot \frac{\psi_{init}}{\frac{1}{S_{init}^2} - 1} \quad (7-8)$$

This can be rearranged as a relation between the hydraulic conductivity (K) and the initial RH for different D values:

$$K(RH_{init}) = \frac{\rho g}{\mu} \cdot k = \frac{\rho g \cdot n \cdot D}{2 \cdot \psi(RH_{init})} \cdot \left(\frac{1}{S_{init}^2} - 1 \right) \quad (7-9)$$

where $\Psi(RH)$ denotes Kelvin's psychrometric law. This function is illustrated in Figure 7-3 which was prepared for the properties of backfill blocks according to Åkesson et al. (2010a). The graphs were made for an initial water content of 17% and a dry density of 1700 kg/m³. An initial RH of 71% and a hydraulic conductivity of 2·10⁻¹⁴ m/s correspond to a diffusivity of 6·10⁻¹⁰ m²/s, which is exactly the same result as in Figure 7-2.

Specific water uptake tests were evaluated with this approach:

An evaluation of MX-80 specimens is shown in Figure 7-4. The specific tests are shown in the top left graph in Figure 5-1 (2 and 4 weeks tests). The hydraulic conductivity for the dry density in question is 5·10⁻¹⁴ m/s according to the adopted curve, and the retention data indicates that the initial RH was 58% for the water content in question. Together, this data set corresponds to a diffusivity level of 4·10⁻¹⁰ m²/s, which is basically the same value as from the direct evaluation of the water-uptake tests in question.

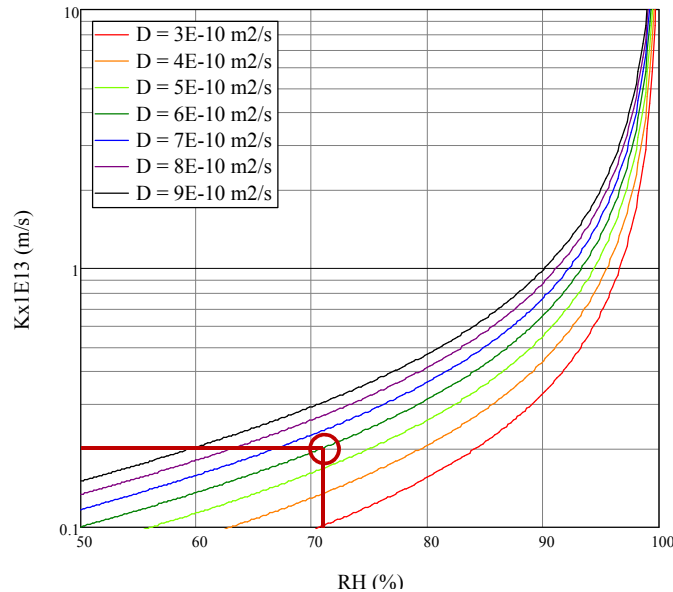


Figure 7-3. Hydraulic conductivity vs. initial RH for different D values. Data corresponding to backfill blocks with MX-80 ($w=17\%$; $\rho_d=1700 \text{ kg/m}^3$; $\rho_s=2780 \text{ kg/m}^3$).

An evaluation of Asha specimens is shown in Figure 7-5. The specific tests are shown in the left middle graph in Figure 5-2 (test 43 & 44). The retention data indicates that the initial RH was 67% for the water content in question, and the directly evaluated diffusivity was $\sim 6 \cdot 10^{-10} \text{ m}^2/\text{s}$. Together, this data set corresponds to a hydraulic conductivity level of $4 \cdot 10^{-14} \text{ m/s}$, and this appears to be consistent with the available hydraulic conductivity data for Asha, although it is in-between results from different studies.

An evaluation of Friedland specimens is shown in Figure 7-6. The specific tests are shown in the right top graph in Figure 5-2 (test 14 & 34). The retention data indicates that the initial RH was 89% for the water content in question, and the directly evaluated diffusivity was $7.8 \cdot 10^{-10} \text{ m}^2/\text{s}$. Together, this data set corresponds to a hydraulic conductivity level of $2 \cdot 10^{-13} \text{ m/s}$ and this appears to be consistent with the available hydraulic conductivity data for Friedland.

An evaluation of specimens with Ibeco RWC BF is shown in Figure 7-7. The specific tests are shown in the left graph in Figure 5-3 (test 23 & 24). The retention data indicates that the initial RH was 72% for the water content in question, and the directly evaluated diffusivity was $5.6 \cdot 10^{-10} \text{ m}^2/\text{s}$. Together, this data set corresponds to a hydraulic conductivity level of $2.3 \cdot 10^{-14} \text{ m/s}$ and this appears to be only slightly lower than the available hydraulic conductivity data for Ibeco RWC BF.

Finally, an evaluation of Febex specimens is shown in Figure 7-8. The specific tests are shown in the Appendix. The retention data indicates that the initial RH was 40% for the water content in question, and the directly evaluated diffusivity was slightly lower than $6 \cdot 10^{-10} \text{ m}^2/\text{s}$. Together, this data set corresponds to a hydraulic conductivity level of $3 \cdot 10^{-14} \text{ m/s}$ and this appears to be fairly consistent with the available hydraulic conductivity data for Febex, although in the lower range.

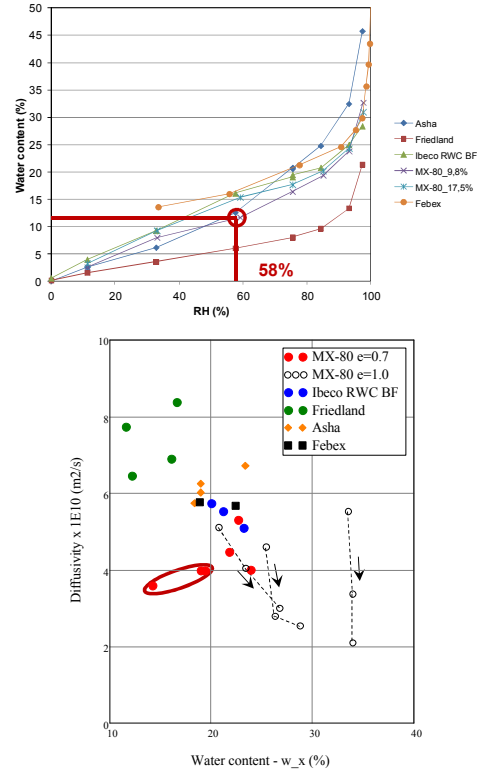
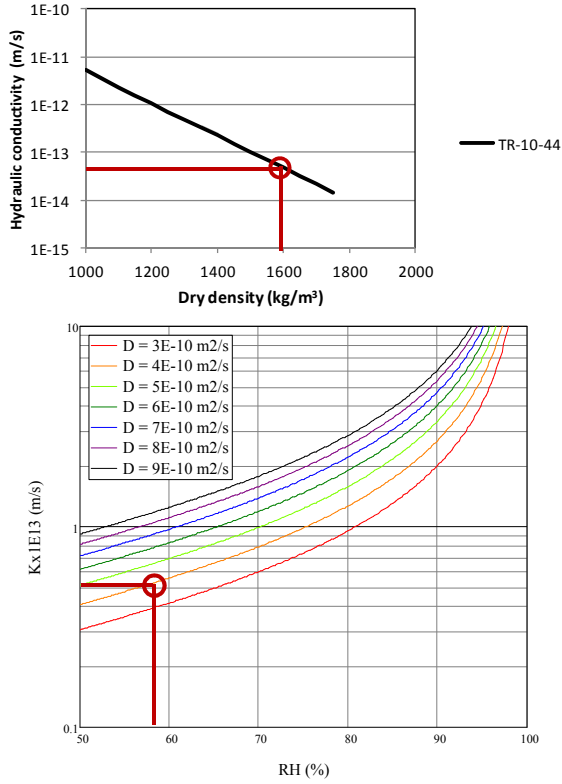


Figure 7-4. Evaluation of water-uptake tests with MX-80 bentonite ($w=11.5\%$; $\rho_d=1590\text{ kg/m}^3$; $\rho_s=2780\text{ kg/m}^3$).

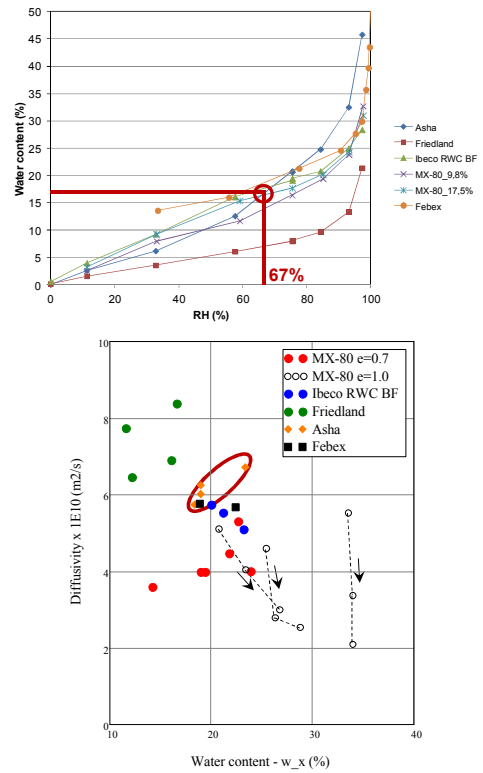
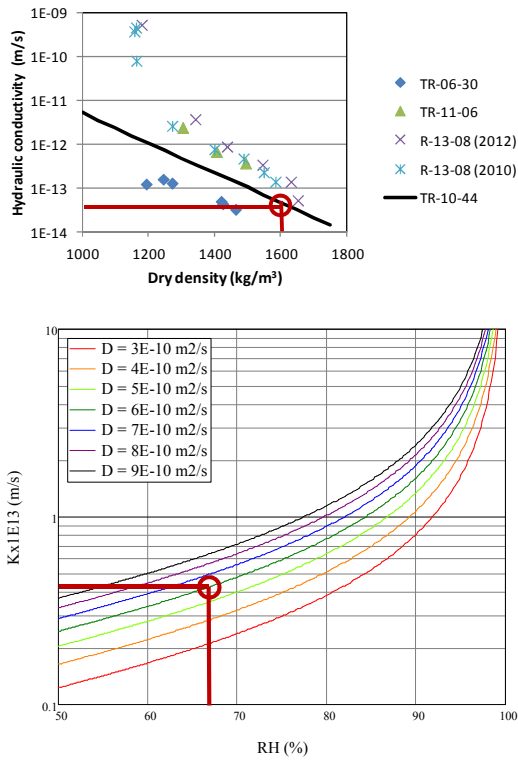


Figure 7-5. Evaluation of water-uptake tests with Asha bentonite ($w=17\%$; $\rho_d=1600\text{ kg/m}^3$; $\rho_s=2900\text{ kg/m}^3$).

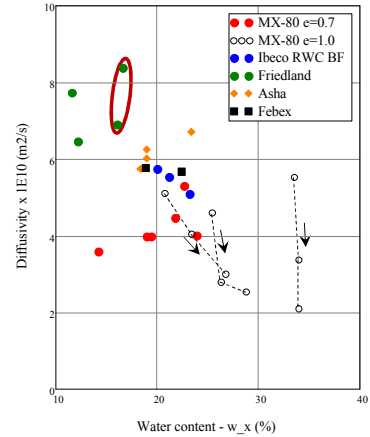
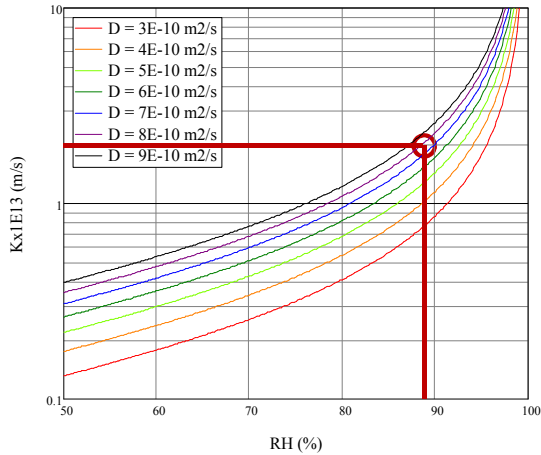
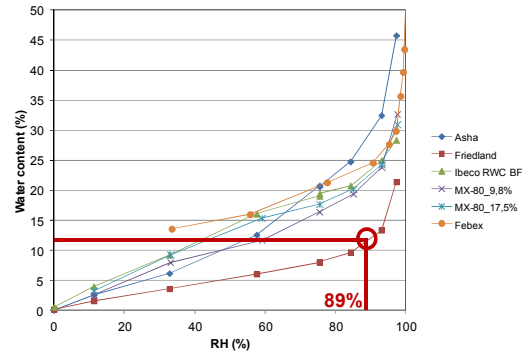
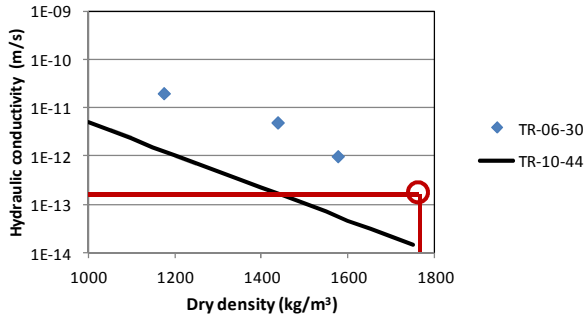


Figure 7-6. Evaluation of water-uptake tests with Friedland bentonite ($w=11.8\%$; $\rho_d=1750$ kg/m^3 ; $\rho_s=2780$ kg/m^3).

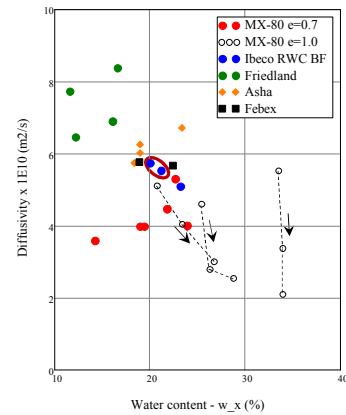
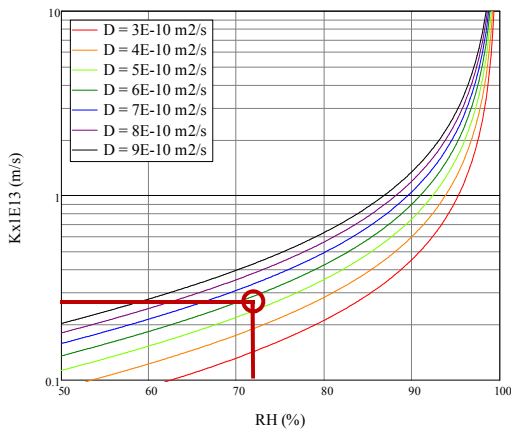
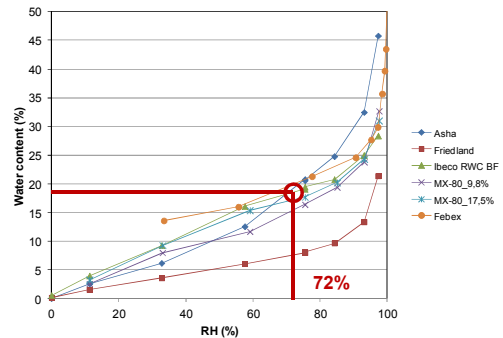
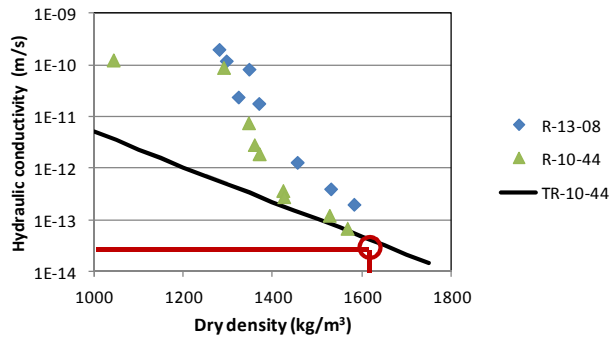


Figure 7-7. Evaluation of water-uptake tests with Ibeco RWC BF bentonite ($w=18.5\%$; $\rho_d=1610$ kg/m^3 ; $\rho_s=2780$ kg/m^3).

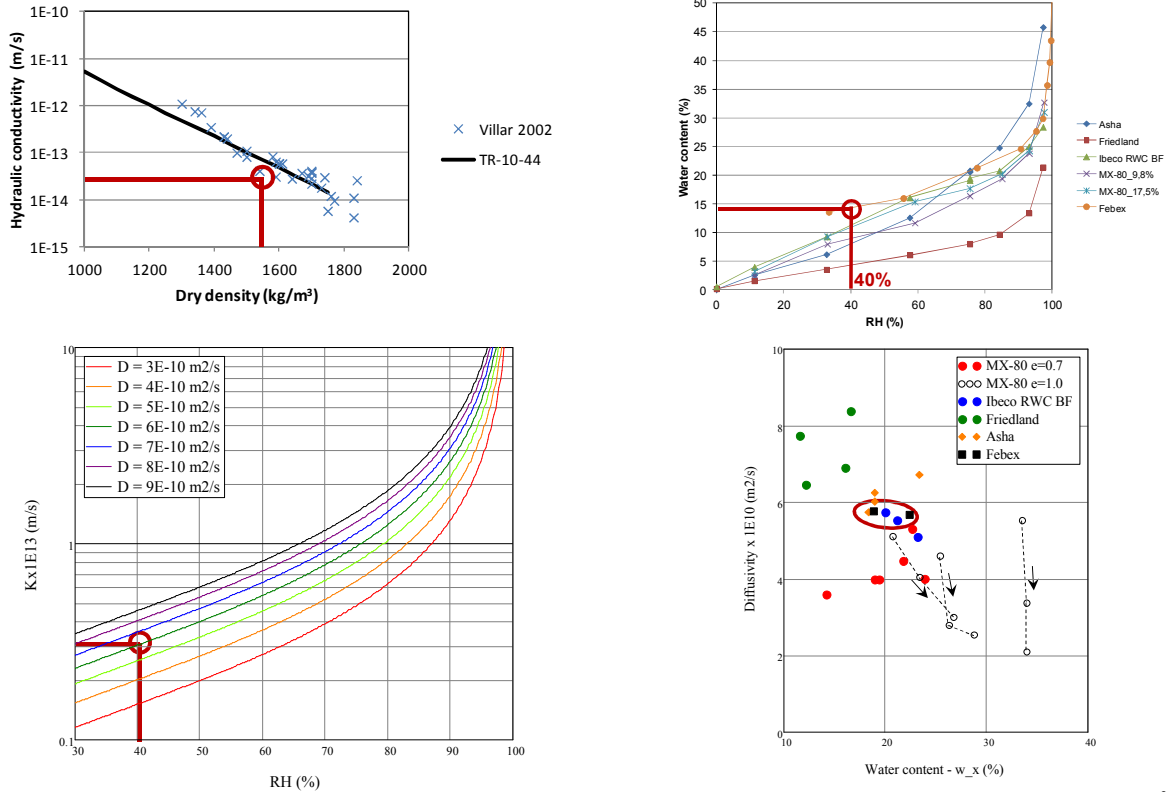


Figure 7-8. Evaluation of water-uptake tests with Febex bentonite ($w=14.3\%$; $\rho_d=1551 \text{ kg/m}^3$; $\rho_s=2753 \text{ kg/m}^3$).

Taken together, this analysis demonstrates a general consistency between the data sets on hydraulic conductivity and retention properties on one hand, and data sets from water uptake tests on the other. It also contributes to a verification of the material model, especially regarding the relative permeability relation ($k_r(S_1)=S_1^3$). Evaluated hydraulic conductivity values which were slightly lower than measured data (Figure 7-7) or in the lower range (Figure 7-8) can be increased by increasing the exponent in the relative permeability law and correspondingly by modifying the retention curve in order to obtain a constant moisture diffusivity value.

8 Homogenization processes

8.1 Homogenization calculations in SR-Site

The THM modeling of buffer, backfill and other system components (Åkesson et al. 2010b) performed for SR-Site included homogenization calculations for the buffer as well as for the backfill. In general, these models consisted of a combination of blocks and pellets and therefore displayed large difference regarding dry density in the initial conditions. Moreover, the FEM program Code_Bright was used for these modeling tasks, and the used constitutive laws were based on the Barcelona Basic Model (Alonso et al. 1990). The sets of parameters which were adopted for these constitutive laws, were based on several types of tests and measurements (Åkesson et al. 2010a): i) compression tests with uniaxial strain at constant suction; ii) swelling tests with uniaxial strain at constant axial load; iii) swelling pressure measurements; iv) shear strength measurements (triax tests); and v) tensile strength measurements (beam tests). Still, all these tests had exclusively been performed on MX-80 bentonite.

Corresponding tests for other materials have basically been limited to swelling pressure measurements (see Chapter 3), although a few shear strength measurements (triaxial tests) have also been performed on specimen with Deponit Ca-N (Dueck et al. 2010). Given the general lack of experimental data, and the inherent uncertainties of the used calculations technique (see Åkesson et al. 2010b), it therefore appears as if a comparison of different material with respect to the homogenization process is currently beyond the horizon, at least by the *means of numerical modelling*. As will be shown in the next section, however, it appears as if *scale tests* can be quite useful for this type of comparisons.

8.2 Homogenization tests

Homogenization tests have been used during the course of different characterizations of backfill candidate materials. These tests are generally performed with a high density compacted specimen (block) in combination with a low density pellets filling in a confined volume, and in which the bentonite can take up water and equilibrate mechanically. Such tests have been performed with different combinations of materials for the blocks and pellets, respectively. Tests performed with one single material for both block and pellets, have so far only been conducted for Ibeco RWC BF (Johannesson et al. 2010) and Friedland (Johannesson et al. 2008). Final void ratio distributions for tests in which the initial thickness of the blocks and pellets was varied are shown in Figure 8-1. These profiles generally display a difference between the highest and lowest void ratio of 0.20 - 0.25 for the tests with Ibeco RWC BF, and correspondingly 0.15-0.30 for the tests with Friedland. This is well in agreement with the backfill homogenizations calculations in SR-Site (Åkesson et al. 2010b), which showed a maximum difference in void ratio of slightly more than 0.2.

The homogenization process is currently a fairly major research topic, with an ongoing project and an associated modelling task within the EBS Taskforce. Still, these activities are limited to saturated conditions, in contrast to the process considered here.

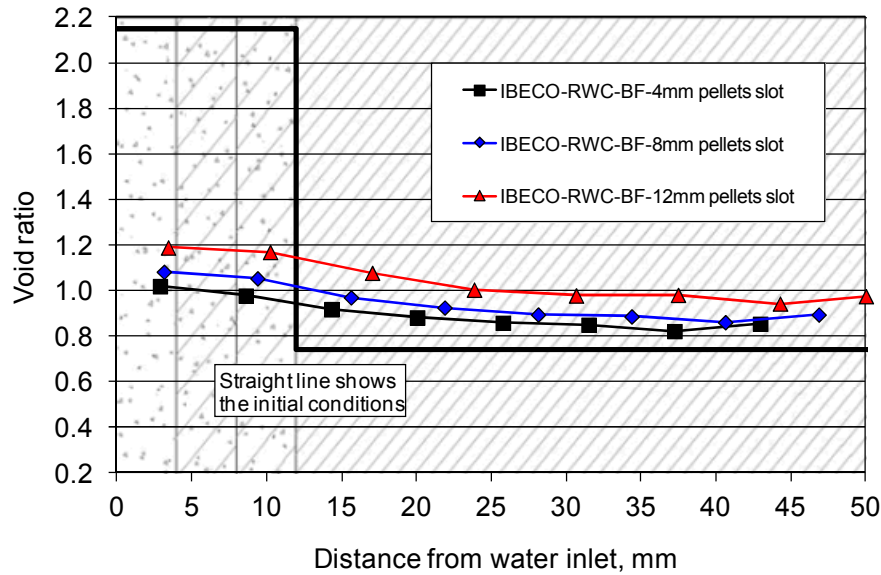
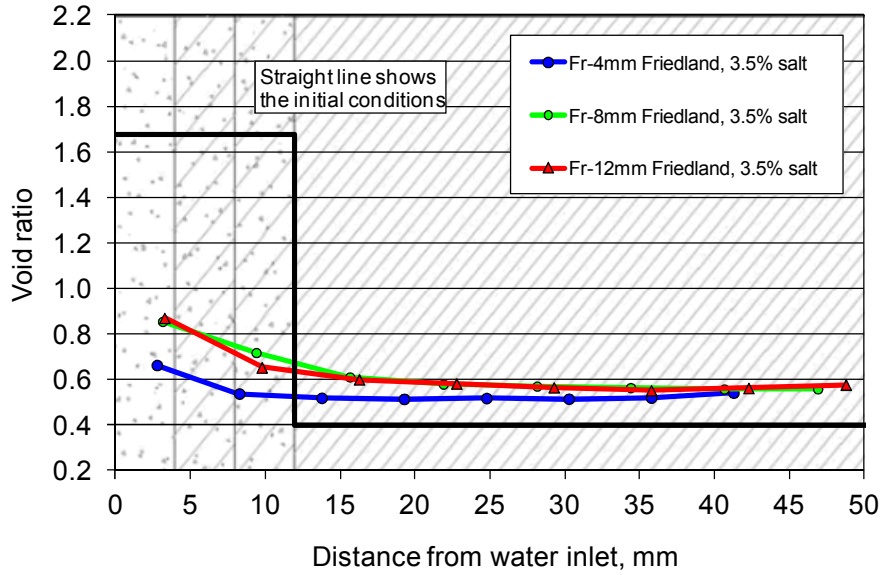


Figure 8-1. Water content (upper), dry density (lower) plotted as function of the distance from the water inlet for the three specimens.

9 Concluding remarks

Time-scale of buffer and backfill hydration

The time-scale of hydration for a certain material is to a large extent determined by the hydro-mechanical properties for the material in question, but also by the initial dry density and water content. In addition, different materials may display optimal properties for different initial conditions. A detailed comparison of different bentonite materials with respect to the time-scale of hydration is therefore not very straightforward. Instead, the evaluated moisture diffusivity data in Figure 7-1 (right) can be used to make a simple comparison of materials. The reason for this is that the time scale of hydration is basically inversely proportional to the diffusivity (e.g. $t_{\text{febex}} \sim t_{\text{mx80}} \cdot D_{\text{mx80}}/D_{\text{febex}}$). Although the variability of the moisture diffusivity was found to be fairly small, it can be noted that the lowest values were found for MX-80. This implies that the time-scale of hydration for other materials would be slightly shorter than for MX-80 (the reduction would be approximately 1/2 for Friedland, and 1/3 for the other analysed materials). Apart from these observations it can be noted that the presented analysis demonstrated a general consistency between the different data sets, and a verification of the material model from independent measurements.

Buffer temperature evolution

The temperature evolution for a certain bentonite material is to a large extent determined by the thermal conductivity for the material in question. Different saturation dependent relations adopted for the thermal conductivity of MX-80 was in this analysis compared with reported data for Febex bentonite. The Febex data is generally quite similar to the MX-80 data relations, although the relations tend to overestimate the thermal conductivity at mid- saturation range, and underestimate the thermal conductivity at low saturation degrees.

Homogenization of buffer and backfill

The homogenization of buffer and backfill was analyzed with THM modeling in SR-Site. These calculations were based on constitutive laws which make use of parameter sets which were adopted from several types of tests and measurements. So far, this has only been performed for MX-80. Given the general lack of experimental data, and the inherent uncertainties of the used calculations technique, it therefore appears as if a comparison of different material with respect to the homogenization process by the *means of numerical modelling* is currently beyond the horizon. *Scale tests*, on the other hand, appears to be a valuable quite simple alternative method which can be used for comparisons of different materials. Scale tests of relevance have generally displayed a difference between the highest and lowest void ratio of 0.20 - 0.25 (Ibeco RWC BF), and correspondingly 0.15-0.30 (Friedland). This is well in agreement with the backfill homogenizations calculations in SR-Site which showed a maximum difference in void ratio of slightly more than 0.2.

References

- Alonso E E, Gens A, Josa A, 1990.** A constitutive model for partially saturated soils. *Géotechnique* **40**, No. 3, 405-430.
- Crank J, 1975.** The mathematics of diffusion. 2nd ed., Oxford University Press, Oxford.
- Dueck A, 2004.** Hydro-mechanical properties of a water-unsaturated sodium bentonite. Laboratory study and theoretical interpretation. Ph. D. Thesis, Lund University.
- Dueck A, Nilsson U, 2010.** Thermo-Hydro-Mechanical properties of MX-80. Results from advanced laboratory tests. SKB TR-10-55, Svensk Kärnbränslehantering AB.
- Dueck A, Börgesson L, Johannesson L-E, 2010.** Stress-strain relation of bentonite at undrained shear. Laboratory tests to investigate the influence of material composition and test technique. SKB TR-10-32, Svensk Kärnbränslehantering AB.
- Börgesson L, 2001.** Compilation of laboratory data for buffer and backfill materials in the Prototype repository. SKB IPR-01-34, Svensk Kärnbränslehantering AB.
- Börgesson L, Åkesson M, Hernelind J, 2013.** 3.2 Analysis of risks and consequences of uneven wetting in a dry deposition hole. SKBdoc 1415878, version 1.0, Svensk Kärnbränslehantering AB.
- Johannesson L-E, Börgesson L, 2002.** Laboratory tests on Friedland Clay. Friedland Clay as backfill material. Results of laboratory tests and swelling/compression calculations. SKB IPR-02-50, Svensk Kärnbränslehantering AB.
- Johannesson L-E, Sandén T, Dueck A, Ohlsson L, 2010.** Characterization of backfill candidate material, IBECO-RWC-BF. Baclo project – phase 3, Laboratory tests. SKB R-10-44, Svensk Kärnbränslehantering AB.
- Johannesson L-E, Sandén T, Dueck A, 2008.** Deep repository-Engineered barrier system. Wetting and homogenization processes in backfill materials. SKB R-08-136, Svensk Kärnbränslehantering AB.
- Kahr G, Kraehenbuehl F, Müller-Vonmoos M, Stoeckli H F, 1986.** Wasseraufnahme und Wasserbewegung in hochverdichtetem Bentonit. Nagra Technischer Bericht 86-14.
- Karnland O, Olsson S, Nilsson U, 2006.** Mineralogy and sealing properties of various bentonites and smectite-rich clay materials. SKB TR-06-30, Svensk Kärnbränslehantering AB.
- Sandén T, Olsson S, Andersson L, Dueck A, Jensen V, Hansen E, Johnsson A, 2013.** Investigation of backfill candidate materials. SKB R-13-08, Svensk Kärnbränslehantering AB (in print).
- Svensson D, Dueck A, Nilsson U, Olsson S, Sandén T, Lydmark S, Jägerwall S, Pedersen K, Hansen S, 2011.** Alternative buffer material. Status of the ongoing laboratory investigation of reference materials and test package 1. SKB TR-11-06, Svensk Kärnbränslehantering AB.
- Villar MV, 2002.** Thermo-hydro-mechanical characterization of a bentonite from Cabo de Gata. A study applied to the use of bentonite as sealing material in high level radioactive waste repositories. ENRESA publicación técnica 04/2002. Madrid.

Åkesson M, Börgesson L, Kristensson O, 2010a. SR-Site data report. THM modelling of buffer, backfill and other system components. SKB TR-10-44, Svensk Kärnbränslehantering AB.

Åkesson M, Kristensson O, Börgesson L, Dueck A, Hernelind J, 2010b. THM modelling of buffer, backfill and other system components. Critical processes and scenarios. SKB TR-10-11, Svensk Kärnbränslehantering AB.

Appendix - Water-uptake tests with Febex bentonite

A.1 General

Water uptake tests were performed in order obtain data on moisture diffusivity for Febex bentonite from independent measurements.

A.2 Test description

The tests were performed as follows:

- Bentonite material with a water content of 14.3% was compacted into cylinders ($\varnothing = 50$ mm and $h = 50$ mm) with a dry density of 1551 ± 1 kg/m³ (void ratio=0.76 and water content at saturation=28% if ρ_s set to 2735 kg/m³, see Svensson et al. 2011)
- The specimens had access to de-ionized water from the bottom during a specified time. The water was not pressurized (less than 10 kPa pressure). During the water uptake the sample was prevented to expand (Figure A.1).
- After the water uptake phase the specimen was removed from the cylinder and the density and water content of the material were determined. The determinations were made on every 10 mm of the specimen. The results from the measurements were plotted as function of the distance from the water inlet.
- Two tests were performed. Test 1 and Test 2 were allowed to take up water during 14 and 21 days, respectively.

A.3 Test results

Results concerning water content and void ratio are shown in Figure A.2 as a function of distance from the water inlet i.e. from the bottom of the specimens. The water content profiles demonstrate that a significant part of the available pore space was filled with water already after the time span of the Test 1. The void ratio distribution confirms that the specimen were fairly homogenously compacted, although the overall void ratio level suggests that the specimen had expanded slightly during the dismantling.

A.4 Final remarks

The tests showed that the Febex bentonite displayed a fairly high capacity for water uptake. The results also showed that the bentonite adjacent to the water inlet tended to expand and therefore displayed relatively high void ratio and water content.

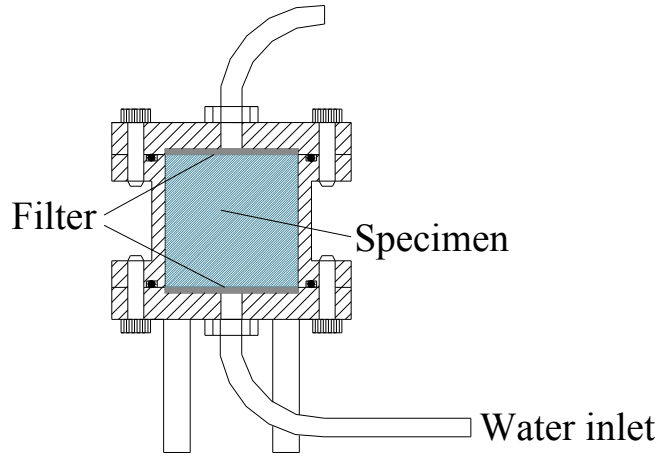


Figure A1. Equipment used for the tests.

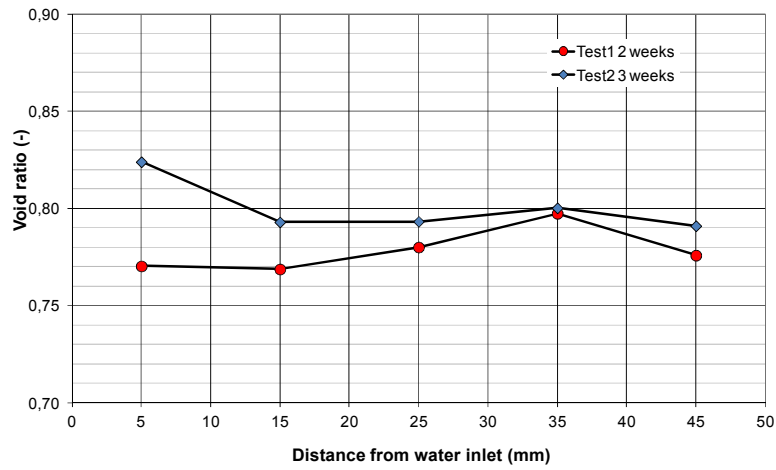
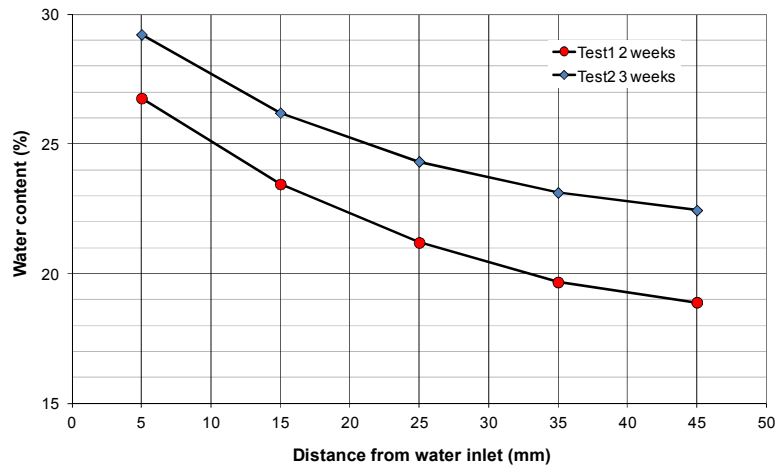


Figure A2. Tests results regarding water content (upper) and void ratio (lower).